

Surface Recombination on the Si(111)2×1 Surface

N. J. Halas and J. Bokor

AT&T Bell Laboratories, Crawfords Corner Road, Holmdel, New Jersey 07733

(Received 29 December 1988)

We have directly monitored population changes in surface states as photoexcited bulk carriers recombine at a semiconductor surface. By observing the time dependence of the density of photoexcited carriers in the conduction band, as well as the transient population in the π^* surface state, a detailed, microscopic model of transient surface recombination is constructed for the Si(111)2×1 surface which includes transient surface-charging effects on the bulk transport self-consistently.

PACS numbers: 73.20.At, 72.20.Jv

Semiconductor surface recombination is presently understood at a phenomenological level in terms of the well known Stevenson-Keyes model¹ with a variety of extensions.² According to this model, surface recombination is a process mediated by trap states which lie in the semiconductor band gap, in analogy with bulk indirect recombination. The direct study of recombination traps by standard photon and electron techniques has thus far not been feasible, but indirect information about such traps can be obtained by a variety of methods.³ Using the recently developed technique of two-photon time- and angle-resolved photoemission spectroscopy, we have, for the first time, succeeded in directly monitoring population changes in surface states as photoexcited bulk carriers recombine at the surface. The surface chosen for this study is the clean, cleaved Si(111)2×1 surface, a surface whose electronic structure is particularly well characterized (refer to Fig. 1). Our observations have allowed us to construct a comprehensive model for recombination on this surface which is consistent with all previously obtained data on its electronic structure,^{4,5} optical properties,⁶ and dynamics.⁷

In this experiment, we have prepared UHV-cleaved

Si(111)2×1 surfaces, and excited a bulk electron-hole plasma using 60-psec pulses of 532-nm visible (pump) radiation. We then directly observed the surface recombination dynamics by monitoring the time dependence of population changes in the surface states as well as the bulk conduction band using time- and angle-resolved photoemission spectroscopy. The experimental apparatus is similar to the one used previously.⁷ Phosphorus-doped Si(111) bars ($\rho=8\ \Omega\text{cm}$, $N_d=3\times 10^{14}\text{cm}^{-3}$), of $3\times 3\text{mm}^2$ cross section, were cleaved *in situ* along the $[2\bar{1}\bar{1}]$ direction. Low-energy electron diffraction (LEED) was used to select single-domain cleaves of the 2×1 reconstruction. Following excitation of the surface with visible pulses at a fluence of 0.5–1.0 mJ/cm², photoemission spectra of both the transiently occupied surface states and the bulk conduction band were obtained using a 60-psec ultraviolet probe pulse, as a function of delay with respect to the pump pulse.

Figure 2 shows the photoemission spectra obtained with 10.5-eV probe radiation on the (a) unpumped and (b) pumped Si(111)2×1 surface. Both spectra were measured at an emission angle of 47°, which corresponds to the \bar{J} point where the π^* surface band reaches its minimum in the surface Brillouin zone (SBZ).⁴ There are two principal features that distinguish the pumped spectrum from the unpumped spectrum, namely, the presence of a photovoltage shift, and the presence of population in the π^* surface state located at $\sim 0.0\text{ eV}$ in spectrum 2(b). Transient population in the π^* surface state has been measured previously using time-resolved photoemission, by direct excitation of the π - π^* transition with 0.45-eV pump radiation.⁷ The spectrum shown here closely resembles case (b) in Ref. 7 where the π and π^* bands are not fully resolved, due to the presence of defect states⁵ in the gap between the π and π^* bands.

The π^* population as seen in Fig. 2(b) has a time dependence which is seen in Fig. 3. For each data point in Fig. 3, a separate photoemission spectrum was recorded with the pump and probe pulses separated by the time indicated on the abscissa. Each spectrum was obtained by integrating for 6000 pump-probe pulse pairs (10-min averaging time), and it is the intensity in the π^* peak that is plotted in Fig. 3. Appropriate care was taken to

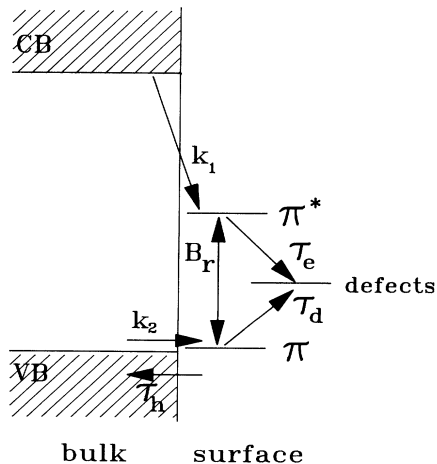


FIG. 1. Schematic diagram of the energy levels and recombination processes for the Si(111)2×1 surface.

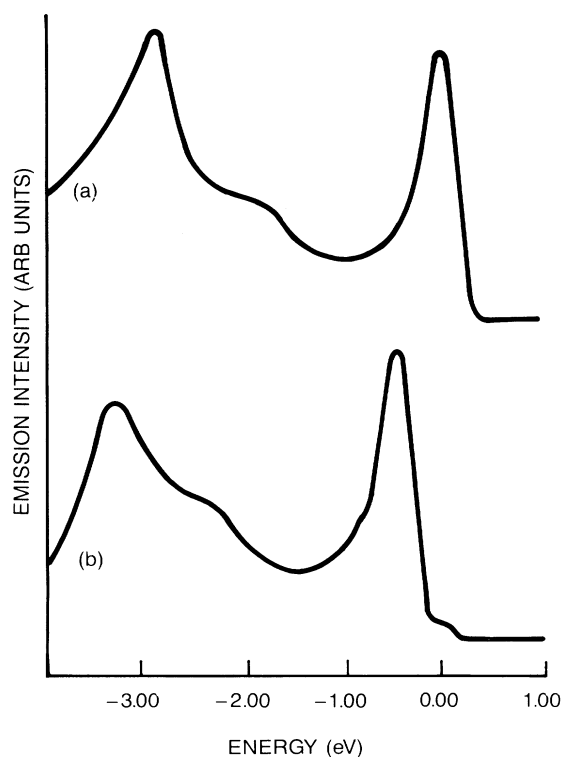


FIG. 2. Photoemission spectra of the Si(111) 2×1 surface, at the \bar{J} point in the SBZ. The zero of energy corresponds to the position of the valence-band maximum on the equilibrium surface. (a) Equilibrium surface; (b) 532-nm-photoexcited surface, at zero time delay between pump and probe pulse.

insure that the surface remained clean during the total time necessary to build up the data.

In addition to the surface state, we monitored the time-dependent density of bulk conduction-band electrons in the near-surface region. In this case, it was previously found⁸ that 4.68 eV is a convenient probe photon energy. We obtained spectra which were virtually identical to that shown in Ref. 8. The time dependence of this photoexcited conduction-band signal was measured for a variety of cleaves and conditions. In particular, the results for a clean and a partially oxidized surface are shown in Figs. 4(a) and 4(b), respectively. The surface used to obtain Fig. 4(b) was prepared by first making a freshly cleaved, single-domain 2×1 surface, and then exposing it to 1000 L [1 Langmuir (L) = 10^{-6} Torrsec] of molecular oxygen just prior to the measurement. The conduction-band peak intensity did not decrease following oxygen exposure, as would be expected for a bulk photoemission peak. The oxidized surface clearly shows a reduced surface-recombination rate relative to the clean surface.

The Stevenson-Keyes model for surface recombination yields an expression for the recombination rate of electron-hole pairs at the semiconductor surface, expressed as a surface-recombination velocity. Assuming a

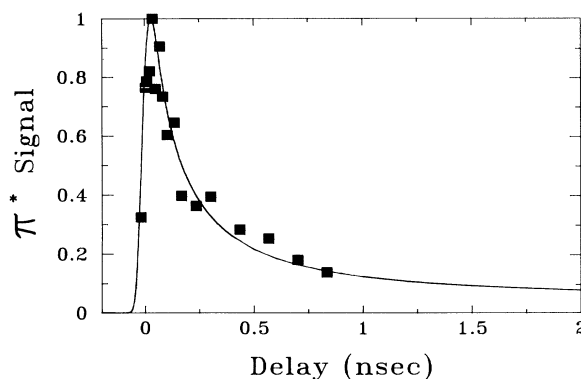


FIG. 3. Time dependence of the π^* -surface-state population, obtained as a function of time delay between photoexcitation and probe pulse.

steady-state condition for the capture and emission of both holes and electrons from the trap states, an expression for the recombination rate per unit area, U , is obtained in terms of capture and emission rates and the carrier densities. The surface-recombination velocity, S , is then usually defined as $U/\Delta n$, where Δn is the density of excess bulk carriers at the surface, or at the boundary between the quasineutral and space-charge regions. Surface recombination can then be naturally incorporated into the description of bulk carrier transport as a boundary condition on the continuity equation. The essence of the Stevenson-Keyes approach is the assumption of steady-state conditions; that is, there is no change in population in the surface state. It is clear, however, that

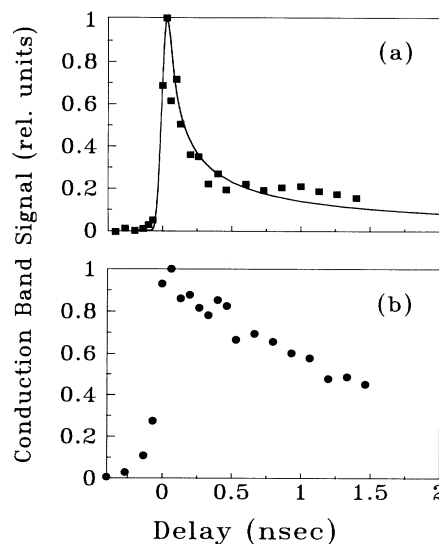


FIG. 4. Conduction-band photoemission as a function of time delay between the photoexcitation and the probe pulse. (a) Clean Si(111) 2×1 surface. (b) Vacuum oxidized Si(111) surface. See text for details of the oxidation process.

our series of measurements occurs in a regime where the charge density in the surface state, as well as the bulk electron and hole density near the surface, is time varying. Indeed, we were unable to obtain an acceptable fit to the data in Fig. 4(a) using the standard solution of the diffusion equation with a surface-recombination boundary condition.⁹ We have therefore made an analysis in which the time-varying space-charge field which arises due to the transient surface-state population is included self-consistently, as are the known specific details of the Si(111)2×1-surface electronic structure. The bulk transport equations for electrons and holes are the continuity equations and Poisson's equation:

$$\frac{\partial n(z,t)}{\partial t} = \frac{\partial J_n(z,t)}{\partial z} = \frac{\partial}{\partial z} \left[n(z,t)q\mu_n E(z,t) + \frac{\mu_n}{kT} \frac{\partial n(z,t)}{\partial z} \right], \quad (1a)$$

$$\frac{\partial p(z,t)}{\partial t} = -\frac{\partial J_p(z,t)}{\partial z} = -\frac{\partial}{\partial z} \left[p(z,t)q\mu_p E(z,t) - \frac{\mu_p}{kT} \frac{\partial p(z,t)}{\partial z} \right], \quad (1b)$$

$$\frac{\partial E(z,t)}{\partial z} = \frac{q}{\epsilon} [p(z,t) - n(z,t) + N_d - N_a], \quad (2)$$

where $n(z,t)$ and $p(z,t)$ are the bulk densities of electrons and holes, $E(z,t)$ is the space-charge field, $J_n(z,t)$ and $J_p(z,t)$ are the electron and hole current densities, μ_n and μ_p are the electron and hole mobilities, q is the charge of the electron, ϵ is the bulk dielectric constant, N_d is the density of donor ions, N_a is the density of acceptor ions, k is Boltzmann's constant, and T is the sample temperature. $G(z,t)$ represents the generation rate of electron-hole pairs by the laser pulse. Since our analysis applies to nanosecond and subnanosecond time regimes, we have neglected the slower process of bulk recombination. We now couple the surface dynamics to the bulk dynamics by imposing the surface rate equations as *boundary conditions* on the above equations. These equations are

$$J_n(0,t) = k_1 \{n(0,t)[N_t - \pi^*(t)] - n_i \pi^*(t) \exp[(E_{\pi^*} - E_i)/kT]\}, \quad (3a)$$

$$J_p(0,t) = -k_2 p(0,t)[N_t - \pi(t)] + \pi(t)/\tau_h, \quad (3b)$$

$$E(0,t) = -(q/\epsilon)[\pi^*(t) - \pi(t) - n_d], \quad (4)$$

$$d\pi^*(t)/dt = k_1 \{n(0,t)[N_t - \pi^*(t)] - n_i \pi^*(t) \exp[(E_{\pi^*} - E_i)/kT]\} - B_r \pi^*(t) \pi(t) - \pi^*(t)/\tau_e, \quad (5a)$$

$$d\pi(t)/dt = k_2 p(0,t)[N_t - \pi(t)] - B_r \pi^*(t) \pi(t) - \pi(t)/\tau_h - \pi(t)/\tau_d, \quad (5b)$$

$$dn_d/dt = \pi^*(t)/\tau_e - \pi(t)/\tau_d. \quad (6)$$

In the above equations, $\pi^*(t)$ and $\pi(t)$ represent the populations of electrons in the antibonding surface state and holes in the bonding surface state, k_1 and k_2 are the respective rate coefficients for capture of bulk electrons and holes, n_d represents the density of electrons occupying surface defect states,⁵ n_i is the intrinsic bulk carrier density, N_t is the total density of bonding and antibonding surface states, and E_{π^*} and E_i are the energies of the π^* -band minimum and the bulk intrinsic energy level above the valence-band maximum, respectively. B_r is the π^* - π recombination coefficient, $1/\tau_h$ is the rate for holes to scatter from the π state to the bulk valence band, $1/\tau_e$ is the rate for electrons to decay from π^* into surface defect states, and $1/\tau_d$ is the rate for holes to decay from π into surface defect states. In Fig. 1, the meaning of the rate constants and lifetimes is indicated schematically. In Eqs. (3b) and (5b), we explicitly use a separate rate, $1/\tau_h$, to describe the rate for hole emission from π back to the valence band rather than the usual detailed-balance argument, such as is used for electron emission from π^* back to the conduction band. This is due to the near-degeneracy between π and the valence-band maximum. In Figs. 3 and 4(a), the solid curves

through the data were obtained by numerically solving¹⁰ Eqs. (1)–(6). We did not attempt this analysis for the oxidized surfaces. In that case, the π^* -surface-state signal is quenched and the recombination dynamics are expected to be completely different. In general, it is known that the surface-state density at the Si/SiO₂ interface is extremely low, and thus very low surface-recombination velocities can be achieved.¹¹

The parameters τ_e , τ_h , and B_r were previously determined,⁷ with some cleave-to-cleave variation in both τ_e and τ_h . In fitting the present data, τ_e and τ_h were allowed to vary within those limits, and the remaining free parameters were k_1 , k_2 , and τ_d . The best fits which we obtained are shown in Figs. 3 and 4 with $B_r = 4 \times 10^{-3}$ cm²/sec, $\tau_e = 200$ psec, $\tau_h = 200$ psec, $k_1 = 3.33 \times 10^{-10}$ cm³/sec, $k_2 = 3.33 \times 10^{-7}$ cm³/sec, and $\tau_d = 1$ nsec. The laser fluence used was 1.0 mJ/cm². The particularly large value required for k_2 to obtain a satisfactory fit is apparently due to the near-degeneracy between the bulk valence-band maximum and the π -state-band maximum.

The model clearly shows the effects of the time-varying space-charge field on the surface-recombination pro-

cess. At the peak of the electron-hole-pair excitation pulse, the surface is depleted of electrons, leaving a net *positive* charge of $\sim 6 \times 10^{12} \text{ cm}^{-2}$. This initial charging of the surface is due to the fact that $k_2 \gg k_1$ as noted above. This surface charge sets up a space-charge region near the surface with a Debye length of $\sim 20 \text{ \AA}$, corresponding to the bulk plasma density of $\sim 4 \times 10^{18} \text{ cm}^{-3}$. The strong fields in the space-charge region lead to an accumulation of bulk electrons in the near-surface region, with a peak value of $7 \times 10^{19} \text{ cm}^{-3}$ at the surface, and a corresponding depletion of holes. It is this accumulation of electrons in the near-surface region that leads to the long tail in the conduction-band signal shown in Fig. 4(a). Because the charge on the surface changes during recombination, the fields in the near-surface region change correspondingly, resulting in a transient band bending (time-dependent surface photovoltage shift) of $\sim 100 \text{ meV}$. This transient band bending is not measurable in our apparatus, due to the fact that the time resolution for measuring a surface potential shift is set by the transit time of the electrons between the surface and the drift-tube entrance. The shift is integrated over this transit time which in our apparatus is $\sim 10 \text{ nsec}$.

It must be emphasized that this self-consistent treatment is necessary to describe adequately the subnanosecond, high-injection case of surface recombination. The rate constants obtained through our data analysis can now be used to describe the low-injection case, where the surface potential remains essentially constant. This steady-state, low-injection limit is the regime addressed by the Stevenson-Keyes model. In this regime, we would predict a surface-recombination velocity of $\sim 3 \times 10^7 \text{ cm/sec}$ for *n*-type $\sim 3 \times 10^4 \text{ cm/sec}$ for *p*-type Si at (111) 2×1 surfaces. The large ratio of recombination velocities between *n*- and *p*-type Si arises from the large ratio k_2/k_1 .

In conclusion, we have directly observed population changes in surface states and in the density of bulk electrons in the near-surface region as a photoexcited electron-hole plasma undergoes surface recombination at

the Si(111) 2×1 surface. We have constructed a detailed and comprehensive microscopic model for this process which includes transient surface-charging effects on the bulk transport self-consistently.

We wish to acknowledge the expert technical assistance of R. H. Storz. We also gratefully acknowledge the assistance of R. Gottscho and N. L. Schryer in the numerical solution of the semiconductor transport equations with nonstandard boundary conditions.

¹D. T. Stevenson and R. J. Keyes, *Physica (Utrecht)* **20**, 1041 (1954).

²For example, P. T. Landsberg and M. S. Abrahams, *Solid-State Electron.* **26**, 841 (1983), and references therein.

³D. E. Aspnes, *Surf. Sci.* **132**, 406 (1983).

⁴R. I. G. Uhrberg, G. V. Hansson, J. M. Nicholls, and S. A. Flodstrom, *Phys. Rev. Lett.* **48**, 1032 (1982); J. E. Northrup and M. L. Cohen, *Phys. Rev. Lett.* **49**, 1349 (1982); P. Martensson, A. Cricenti, and G. V. Hansson, *Phys. Rev. B* **32**, 6959 (1985).

⁵N. J. DiNardo, J. E. Demuth, W. A. Thompson, and Ph. Avouris, *Phys. Rev. B* **31**, 4077 (1985).

⁶P. Chiaradia, A. Cricenti, S. Selci, and G. Chiarotti, *Phys. Rev. Lett.* **52**, 1145 (1984); M. A. Olmstead and N. M. Amer, *Phys. Rev. Lett.* **52**, 1148 (1984).

⁷J. Bokor, R. Storz, R. R. Freeman, P. H. Bucksbaum, *Phys. Rev. Lett.* **57**, 881 (1986).

⁸J. P. Long, R. T. Williams, J. C. Rife, and M. N. Kabler, in *Energy Beam-Solid Interactions and Transient Thermal Processing*, edited by D. K. Biegelsen, G. A. Rozgonyi, and C. V. Shank, MRS Symposia Proceedings No. 35 (Materials Research Society, Pittsburgh, 1984), p. 81.

⁹M. S. Tyagi, J. F. Nijs, and R. J. Van Overstraeten, *Solid-State Electron.* **25**, 441 (1982).

¹⁰N. L. Schryer, "Designing Software for One Dimensional Partial Differential Equations" (to be published); Bell Laboratories (Murray Hill, NJ) Computing Science Technical Report No. 115, 1984 (unpublished).

¹¹S. Kar and R. L. Narasimhan, *J. Appl. Phys.* **61**, 5353 (1987); E. Kamieniecki, *J. Appl. Phys.* **57**, 2840 (1985).